Quantum Monte Carlo study of few-electron concentric double quantum rings

Leonardo Colletti,[1,2] Francesc Malet,[3] Marti Pi,[3] and Francesco Pederiva[4]
[1]*INFN-Gruppo Collegato di Trento, via Sommarive, 14, 38100 Trento, Italy*
[2]*Free University of Bolzano, via Sernesi, 1, 39100 Bolzano, Italy*
[3]*Departament ECM, Facultat de Fisica and IN^{2}UB, Universitat de Barcelona, Diagonal 647, 08028 Barcelona, Spain*
[4]*Dipartimento di Fisica, Universitá di Trento, via Sommarive, 14, 38100 Trento, Italy and INFM-DEMOCRITOS National Simulation Center, 34014 Trieste, Italy*
(Received 2 October 2008; revised manuscript received 21 January 2009; published 17 March 2009)

We consider few-electron concentric double quantum rings with parabolic confining potential and compare the ground-state energies calculated by exact diagonalization of the Hamiltonian, accurate quantum Monte Carlo, and local spin-density functional approaches. Electronic localization in one of the rings and the formation of rotating Wigner molecules is shown, respectively, from the one-body and the two-body density operators. As the confinement strength of the outer ring is finely increased, the circularly symmetric electron density exhibits a radial crossover from this ring to the inner one without altering the angular character of the system.

DOI: 10.1103/PhysRevB.79.125315 PACS number(s): 73.21.−b, 73.22.Gk

I. INTRODUCTION

Double quantum rings are natural follow-ups of structures such as quantum dots (QDs) and quantum rings (QRs), which have been the subject of intense both theoretical and experimental studies for the past ten years, see, e.g., Refs. 1–5 and references therein. All these structures are characterized by Coulombic correlations enhanced by electron densities much lower than those of their natural counterparts, i.e., electrons confined in atoms. Here we consider concentric double quantum rings (CDQRs) (Refs. 6–8) containing $N=2-4$ electrons and, owing to their formal resemblance–both kinds of systems have a central potential, we adopt the atomic jargon by referring to the two-, three- and four-electron systems as helium, lithium, and beryllium CDQRs, respectively.

As an important difference with respect to atoms, QDs may show a wealth of properties (energy spectrum,[9] total spin,[10] electron localization,[11,12] conductance, etc.) that are tunable by the variation of a set of experimentally controllable parameters such as the shape, the depth and the size of the external confinement, the number and the density of the electrons, the presence of impurities[13,14] or the intensity of an external magnetic or electric field, making them a promising playground for the development of nanotechnological devices. Similar properties are displayed by QRs (Ref. 15) and coupled systems such as QD-QD,[16] QR-QR,[17] or QD-QR (Ref. 18) pairs, in which case the set of tunable parameters is further expanded, since one can change the size, shape, and position of the constituents relative to each other.

Being strictly connected to the strength of the electronic correlations, a correct description of these properties crucially depends on the accurate theoretical treatment of the underlying many-body problem. To this end, in the investigations described here we make use of an up-to-date quantum Monte Carlo (QMC) approach and compare the obtained results with those calculated within a local spin-density approximation (LSDA) one and with exact diagonalization (ED) techniques. QMC is known for having been able to provide benchmark results for a variety of systems,[19] although in the fermionic case they are affected by the fermion node problem,[20] which can be, in turn, systematically reduced.[21] The LSDA has also established itself as the standard tool for atomic-scale simulations and has been proved to satisfactorily describe from few- to many-electron QDs, QRs, and CDQRs.[4,5,22] ED essentially allows for the exact solution of the Schrödinger equation, but it is practically feasible only for systems with a small number of particles.[23]

We have calculated the ground-state (g.s.) energy for fixed radii of the rings and various strengths of the external confinement, as well as the ordinary—one-body— and two-body densities. The latter is also often referred to as[24,25] conditional-probability distribution (CPD) and represents a fundamental tool to reveal crystallization in the system when measured from the intrinsic frame of reference—i.e., from the position of one of the electrons. Indeed, it may happen that this quantity shows accumulation of electronic density in specific spots of the system whereas from the outside—laboratory frame—the ring presents rotational symmetry via the one-body density. We have adopted a variational Monte Carlo (VMC) method in which the trial wave function is carefully optimized with respect to the energy rather than to the energy variance,[21,26] thus providing a very accurately chosen sample of configurations for the subsequent diffusion Monte Carlo (DMC) study; Sec. II summarizes the theoretical model; Sec. III presents overall results that are then commented in depth in subsections for each case of study and, finally, in Sec. IV we draw some conclusions as well as some anticipations of further studies.

II. CDQR MODEL

We consider N electrons confined in the two-dimensional quantum well formed at the interface of a semiconductor GaAs/AlGaAs heterostructure, and further confined by a double harmonic central potential[18,27] with the two minima located at distances R_{in} and R_{out} from the origin and confinement strengths ω_{in} and ω_{out}, namely,

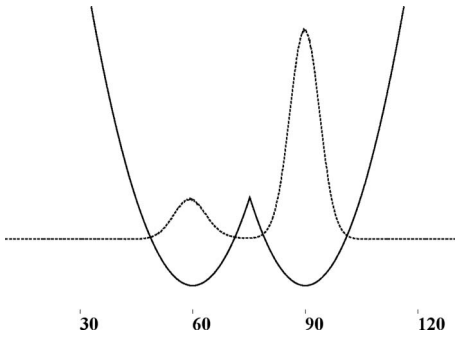

FIG. 1. Solid line: cross section of the circularly symmetric potential (R_{in}=60 nm, R_{out}=90 nm, ω_{in}=35 meV, ω_{out}=36 meV). Dashed line: The VMC-calculated density profile (for N=3). The y axis is in arbitrary units, x axis in nm.

$$V_{conf}(r) = \min\left[\frac{1}{2}m^*\omega_{in}^2(r-R_{in})^2, \frac{1}{2}m^*\omega_{out}^2(r-R_{out})^2\right], \tag{1}$$

m^* being the effective electron mass. This confining potential is shown in Fig. 1 as a function of r, together with the density profile, calculated by VMC, corresponding to one of the studied configurations with N=3.

The Hamiltonian reads

$$\hat{H} = \sum_{i=1}^{N}\frac{\mathbf{p}_i^2}{2m^*} + V_{conf}(\mathbf{r}_i) + \sum_{i<j}^{N}\frac{e^2}{\epsilon|\mathbf{r}_i-\mathbf{r}_j|}, \tag{2}$$

where $\mathbf{p}_i$ and $\mathbf{r}_i$ are, respectively, the momentum and position of the ith electron. We adopt millielectronvolts (meV) and nanometers (nm) for the quantification of the confinement's strength and radii, whereas for the ground-state energies and density-distribution radii we employ effective atomic units. We take the effective mass m^*=0.067 and dielectric constant ϵ=12.4 values of bulk GaAs. In effective atomic units $\hbar=e^2/\epsilon=m=1$, which yields for the effective Hartree and Bohr radius the values H^*=11.86 meV and a_B^*=9.79 nm, respectively.

III. RESULTS

We have studied systems with N=2, 3, and 4 interacting electrons in a geometry with fixed parameters R_{in}=60 nm, R_{out}=90 nm, and ω_{in}=35 meV, and with variable ω_{out}. The usual parameter $r_s=1/\sqrt{\pi n}$ (in a_B^* units), n being the electron density, has been used in order to characterize the systems under study, ranging from 2.5 to 4.3, i.e., values well below both the typical ones at which Wigner crystallization appears in the two-dimensional electron gas (r_s about 37, Ref. 28) and in QDs (r_s about 20, Ref. 11).

Concerning the QMC calculation, the employed trial wave functions have been obtained after accurate cycles of energy-optimized VMC runs and contain the usual determinantal part, accounting for the total antisymmetry required by fermion systems and a Jastrow factor which includes the two- and three-body correlations. Only the parameters contained in the Jastrow part underwent the optimization procedure. This turned out to be sufficient to guarantee a good convergence of DMC energies to ED ones. In order to retain the symmetry with respect to the spin, the determinants (one for spin-up and another for spin-down electrons) are made up of single-particle (sp) orbitals obtained from a local-density approximation (LDA) calculation. For details on the form of the wave function and on the optimization algorithm, see Umrigar *et al.*[21] and references therein. The DMC results are obtained by long runs repeated by varying both the time step (δt=0.05, 0.035, 0.02, and 0.01) and the number of walkers (N_{walk}=100, 200, 300, and 400) in order to extrapolate the ground-state energy quadratically for $\delta t \to 0$ and linearly for $1/N_{walk} \to 0$. DMC two-body densities have been obtained by collecting relative distributions of electrons on a mesh of a set of at least 500 000 configurations sampled from the ultimate distribution to which the algorithm converges in the limit of long simulation times.

Finally, for the exact diagonalization we have performed configuration interaction calculations building the Slater determinants from LSDA single-particle orbitals instead of, e.g., Fock-Darwin states in order to ensure a better convergence.[29] Such sp states are written in the usual form $\varphi_{nl\sigma}(\mathbf{r},\sigma)=u_{nl\sigma}(r)e^{-il\theta}\chi_\sigma$, with $n=0,1,2,\ldots$, $l=0,\pm1,\pm2,\ldots$, $-l$ being the projection of the sp orbital angular momentum on the z axis and $\sigma=+1/2(-1/2)$ referring to spin-up (-down) states. Thus, the many-body wave function with given total z component of the spin S_z and angular momentum $L_z=\Sigma_i l_i$, Ψ_{S_z,L_z}, is expressed as a linear combination of Slater determinants $\Phi^\alpha_{S_z,L_z}$, namely, $\Psi_{S_z,L_z}=\Sigma_\alpha c_\alpha \Phi^\alpha_{S_z,L_z}$. We have considered large numbers of configurations (α's up to 500 000) checking that the obtained ground-state energies tend asymptotically to the value that would correspond to the limit $\alpha=\infty$. The integrals entering the calculation of the Coulomb matrix elements have been performed using a step of h=0.02 a_B^*, and to solve the secular equation $(\hat{H}-E_{L_z,S_z}\mathcal{I})\Psi_{S_z,L_z}=0$, where $\mathcal{I}$ is the identity matrix, we have used the Lanczos package ARPACK,[30] which was designed to address eigenvalue problems dealing with large sparse matrices.

For all the CDQR configurations presented here, the one-body density shows azimuthally delocalized and radially localized electrons. On the two-body density level of investigation, the electrons are localized, giving rise to a unique, intrinsic angular modulation of the particle densities, analogous to the *rotating electron molecules* found in boson traps.[24] Concerning the ground-state energy estimations, DMC and ED show a good agreement. DMC and ED one-body and two-body densities result practically indistinguishable: in most cases this convergence is fully quantitative, while in some cases (for values of ω_{out} in the crossover region) it is only qualitative, with the two methods yielding the same shape but different relative heights of the density peaks. Nevertheless, for the sake of clarity, only DMC densities are reported in all figures. On the contrary, as it is expected and well known, the LSDA overestimates the correlation energy. This, as we shall see, is clearly manifested as a difference between the LSDA and the DMC/ED energies and densities that is enhanced for the lowest values of the density, i.e., for the situations with the smallest number of

TABLE I. Comparison of the ground-state energies of the helium CDQR corresponding to different values of the confinement of the outer ring. The uppercase labels "IN" and "OUT" indicate the ring in which the electrons are mostly localized.

ω_{out} (meV)	LSDA (H^*)	VMC (H^*)	DMC (H^*)	ED (H^*)
35.15 (IN)	2.9499	3.04694(9)	3.0113(5)	3.0213
35.14 (OUT)	2.9035	3.0309(1)	3.0222(1)	3.0209

electrons and increasing when they are localized in the outer ring.

A. $N=2$ (helium) CDQR

We have first investigated the electron localization in a CDQR containing two electrons as a function of the variable confinement strength of the outer ring. As shown below, the QMC (DMC) results are very close to the ED ones, the discrepancy being on the order of 1 to 10 mH^* and thus in good agreement with analogous comparisons performed on same-scale systems,[23,31] whereas they differ significantly from those obtained within the LDA, which in this case coincide with the LSDA ones since the two electrons pair as a singlet, as expected.[32] We also point out that for this system, characterized by a zero total spin, the space part of the wave function has to be symmetric, thus implying that the DMC algorithm converges to the exact ground state energy within the statistical error, therefore resulting in a reliability test of the ED approach. Table I shows the calculated ground-state energies, and one can see that the LSDA ones are systematically lower than those given by QMC, the latter being an upper bound. The difference between the two approaches is fundamentally related to the non-variational nature and the above-mentioned overestimation of the correlation energy in the density-functional approach. Such difference increases from a 3% to a 4.3% of the total DMC energy as the density reduces (i.e., as the correlations become more important), which corresponds to the electrons moving from the inner ring ($\omega_{out}=40$ meV) to the outer one ($\omega_{out}=30$ meV). The corresponding electron density profiles are shown in Fig. 2, where also remarkable differences between the different calculations can be observed. Indeed, one can see that whereas both in the LDA and in the VMC ones a sudden crossover from the situation in which the two electrons are completely localized in the outer ring to that in which they are in the inner ring takes place as the strength of the confinement of the outer ring is increased from $\omega_{out}=35.14$ meV to 35.15 meV, such transition is more continuous in the DMC calculation. It could also be interpreted as an artifact of the LDA and the VMC approaches due to the abrupter character shown in these calculations. The sudden crossover is somewhat a drawback of the LDA and the VMC due to a poorer description of electron-electron correlations. DMC cures this shortcoming, producing a smoother transition from one ring to the other. Figure 3 displays how does the magnetization $\rho(r,\uparrow)-\rho(r,\downarrow)$ of the CDQR vary as the displacement of the electronic density to the outer ring becomes energetically

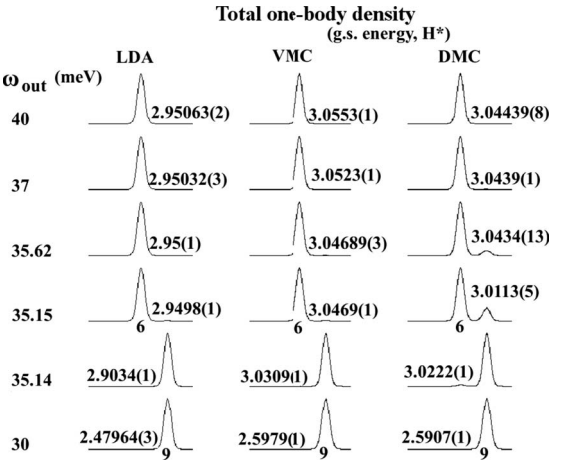

FIG. 2. Comparison of electron densities of the CDQR with $N=2$ calculated within the LDA and the QMC approaches. The position of the peaks on the x axis is given in a_B^* and the value of the total energy is indicated in each plot; the y axis is in arbitrary units. ω_{out} indicates the confinement's strength of the outer ring.

favorable when the confinement's strength ω_{out} is finely reduced, indicating that the crossover of the total density begins by a slight separation of the two spin-resolved one-body densities. The amount by which the two densities differ on each ring is about 10% of the total density for $\omega_{out}=35.62$ and decreases as the confinement's strength is lowered and both electrons can be fully allotted in the same, outer ring. This effect is not present in the LSDA results, suggesting that it is due to subtle correlations between the electrons which can be correctly treated only by exact methods (DMC and/or ED). The IN-OUT transition is displayed in a more detailed way in Figs. 4 and 5, where the one- and two-body densities and the relative angular localization of the electrons corresponding to the two configurations discussed in Table I are shown for the VMC and the DMC approaches, respectively. The latter yields a more continuous redistribution process of the electron density between the two constituent rings as the

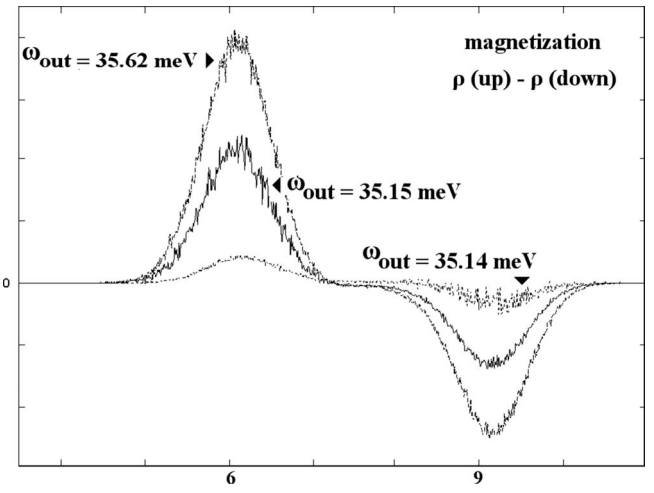

FIG. 3. DMC-calculated magnetization for CDQR with $N=2$ as a function of the radius (x axis in a_B^*, y axis in arbitrary units). ω_{out} indicates the confinement's strength of the outer ring.

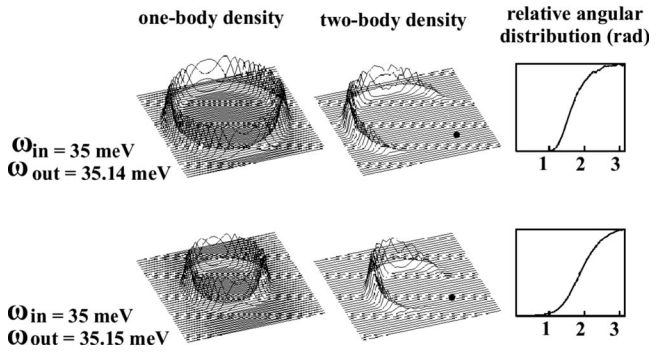

FIG. 4. VMC results for the helium CDQR. Top panels: $\omega_{out}=35.14$ meV; Bottom panels: $\omega_{out}=35.15$ meV. Left: one-body density; center: two-body density, the dots indicating the position of the reference electron; right: relative angular distribution in arbitrary units (x axis in radians).

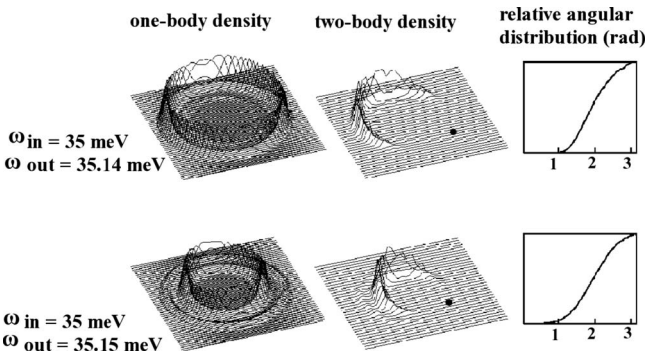

FIG. 5. Same as Fig. 4 for the DMC calculation.

critical ω_{out} is reached, as it is illustrated in the left panels of both figures. The central panel shows the two-body density $\rho(r,r_1)$, i.e., the conditional probability of finding the second electron at the position r when the first electron is fixed at r_1; a more quantitative information is presented in the right panel, where the displacement probability of the second electron with respect to the first one is shown as a function of the angle formed by the position vector of the two electrons. It can be seen that the particles are preferably located forming a relative angle of 180° to minimize the Coulomb energy.

B. $N=3$ (lithium) CDQR

We must recall here a general remark: ED and LSDA results on one side, and QMC ones on the other, cannot be strictly compared due to the fact that while QMC can treat eigenstates of $\hat{S}$, LSDA and our ED algorithm are limited to eigenstates of $\hat{S}_z$. As a consequence, e.g., the state with eigenvalue $S_z=0$ resulting from an ED or LSDA calculation is a mixture of the $S=0$ and $S=1$ states. To build proper VMC projection functions and DMC trial wave functions by using LDA states we made use of the Dirac identity (see e.g., Colletti *et al.* in Ref. 10). The ground-state energies for the $N=3$ CDQR are shown in Table II. For the inter-ring separations we have explored, the ground state of the system is found to be fully spin-polarized, i.e., $S=3/2$ by QMC and $S_z=3/2$ by LSDA, in agreement with Herring,[32] Usukura *et al.*[33,34] and Mikhailov,[35] whereas ED yields $S_z=1/2$. To allow a thorough comparison and a check of the validity of Hund's (first) rule in CDQRs, we calculated in one case ($\omega_{out}=40$ meV) the QMC energy for the state with $S=1/2$, which results by a 0.3% higher than the ground-state energy. Ground-state energy differences between the results given by the ED and the QMC calculations are of the order of $3-5\ mH^*$. The LSDA overestimation of the correlation energy increases in this case from a 1.8% to a 5% of the total DMC energy as the density reduces when the electrons move from the inner ring ($\omega_{out}=40$ meV) to the outer one ($\omega_{out}=34$ meV). In analogy with the findings for $N=2$, as the outer confinement strength is increased the electron density appears to sharply crossover from the outer to the inner ring in the LSDA and in the VMC calculation, whereas the DMC one yields a smoothed out transition as before, as shown in Fig. 6. It must be noticed that for $\omega_{out}=35.5$ meV the LSDA yields a configuration with the three electrons localized in the inner ring whereas in the QMC calculation (both in VMC and DMC) they are mostly in the outer one. The relative angular distribution and the two-body density correlation function are shown in Fig. 7, from where one can see that in this case the electrons tend to localize forming an equilateral triangle within the CDQR—i.e., at relative angles of around 120°—regardless of whether they are in the inner ring or in the outer one. This character of the two-body density, which essentially represents a symmetry breaking of the density in the intrinsic, rotating, frame can be interpreted as the molecular counterpart of the Wigner crystallization occurring in

TABLE II. Same as Table I for the lithium ($N=3$) CDQR. For the particular case $\omega_{out}=35.5$ meV the label "IN" corresponds to the LSDA calculation, and the label "OUT" to the QMC one. Comparison of first and last row suggests that electrons in a CDQR structure obey Hund's (first) rule.

ω_{out} (meV)	LSDA (H^*) $S_z=3/2$	VMC (H^*) $S=3/2$	DMC (H^*) $S=3/2$	ED (H^*) $S_z=1/2$
40 (IN)	4.681	4.76603(7)	4.76482(8)	4.7681
36 (IN)	4.567	4.7743(1)	4.7441(5)	4.7488
35.5 (IN/OUT)	4.5668(1)	4.7111(1)	4.6989(5)	4.7042
35.495 (OUT)	4.4746	4.7104(1)	4.6932(9)	4.7031
34 (OUT)	4.291	4.5213(5)	4.51695(8)	4.5198
40 (IN)		$S=1/2$ 4.7825(9)	$S=1/2$ 4.7692(1)	

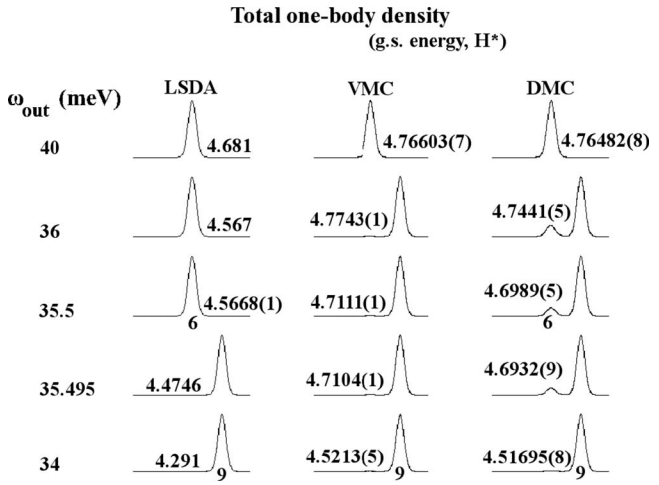

FIG. 6. Same as Fig. 2 for the lithium ($N=3$) CDQR.

low-density electron systems[11] and by analogy such azimuthal modulation can be referred to as a *Wigner molecule*. One should also notice differences with what could be interpreted at first sight as the appearance in the system of the so-called charge-(CDWs) and spin-density waves (SDWs) found in quantum dots,[36] which involve the one-body rather than the two-body density, but in which the number of humps does not coincide with the number of particles.[37] This may lead one into considering the CDWs as having a physical nature different from that of the Wigner (ordinary or molecular) crystallization; such SDWs have been considered by some authors as an artifact of the LSDA.[38]

C. $N=4$ (beryllium) CDQR

Also for $N=4$ a thorough comparison between ED and QMC results is limited by the multiplicity of S_z with respect to S. The energies for the $N=4$ system in the ED- and LSDA $[L=0,S_z=0]$ state and QMC $[L=0,S=0]$ are shown in Table III. As we explain below, this configuration is found to be the ground state from the ED calculation, but not from the LSDA and the QMC ones. Discrepancies between ED and QMC are of the same order as in the previous cases (1 to 12 mH^*), thus remaining within the range found for QDs by other authors.[23,31] For the CDQRs with the largest number of

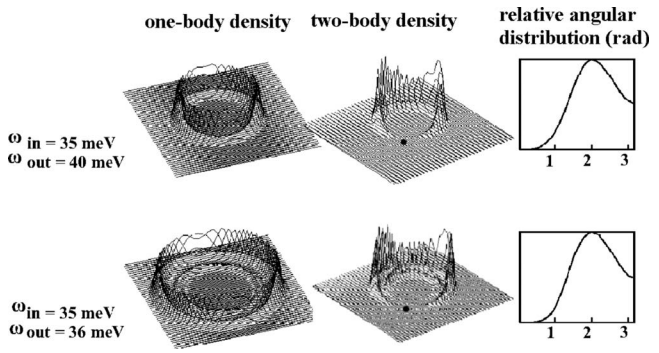

FIG. 7. Same as Fig. 5 for the CDQR with $N=3$. Top panels: $\omega_{out}=40$ meV; bottom panels: $\omega_{out}=36$ meV.

TABLE III. Same as Table I for the beryllium ($N=4$) CDQR. Energies refer to the $[L=0,S_z=0]$ state for LSDA and ED, and to the $[L=0,S=0]$ state for VMC and DMC.

ω_{out} (meV)	LSDA (H^*)	VMC (H^*)	DMC (H^*)	ED (H^*)
40 (IN)	6.6080(1)	6.721(4)	6.66199(2)	6.6628
37.5 (IN)	6.4461(1)	6.759(2)	6.6714(10)	6.6595
35 (OUT)	6.2408(1)	6.4179(5)	6.3868(5)	6.3897

electrons considered, we have found that the LSDA overestimates the correlation energy by a percentage that increases from a 0.8% to a 2.2% of the total DMC energy as the density reduces with the particles moving from the inner ($\omega_{out}=40$ meV) to the outer ring ($\omega_{out}=35$ meV), in agreement with the results obtained in the previous subsections. It should be noticed that, as anticipated above, this overestimation clearly shows a tendency to decrease as N increases, which illustrates the well-known fact that the LSDA is less reliable for systems containing a very small number of particles. Figure 8 shows the comparison between the radial densities calculated within the LSDA and the QMC approaches. Indeed, one can see that the LSDA densities resemble more the QMC ones than in the previous ($N=2$ and 3) cases, showing now a smoother transition of the radial electronic distribution from the inner to the outer ring. For the $[L=0,S=0]$ case we have calculated the DMC spin-dependent two-body density $\rho(r_\sigma,r_{1\sigma'})$, which represents the conditional probability of finding a spin-σ electron at the position r provided that a spin-σ' electron is fixed at the position r_1. One-body and two-body spin-dependent densities are shown in Fig. 9. Clear peaks can be observed, showing that like-spin electrons tend to be distributed in the rings forming a $\pi/2$ rad angle, whereas antiparallel-spin particles tend to arrange in opposite positions (i.e., forming a π rad angle) though obviously they can also form a $\pi/2$ rad angle since $N=4$. Hence, the electrons are distributed in an up-up-down-down sequence along the ring, yielding a ground state formed by two like-spin and two antiparallel-spin nearest-neighbor pairs. This picture is confirmed by Fig. 10, in which the angular modulations corresponding to the panels of Fig.

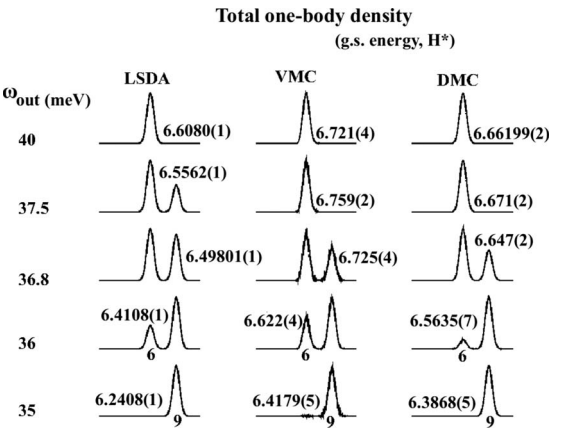

FIG. 8. Same as Fig. 2 for the CDQR with $N=4$.

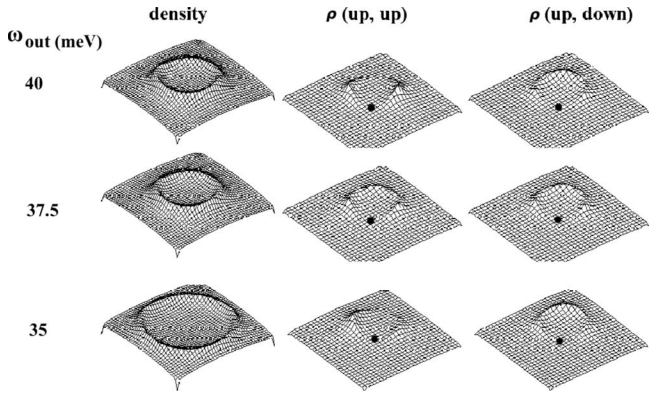

FIG. 9. DMC results for the beryllium CDQR ($N=4$). Top panels: $\omega_{out}=40$ meV; middle panels: $\omega_{out}=37.5$ meV; bottom panels: $\omega_{out}=35$ meV. Left: one-body density; center: two-body density $\rho(r_\uparrow;r_\uparrow)$, right: two-body density $\rho(r_\uparrow,r_\downarrow)$. The dots indicate the position of the reference electron.

9 are shown. For this system we have also calculated the DMC spin-dependent three-body distribution function $\rho(r_\sigma,r_{1\sigma'},r_{2\sigma'})$, which gives the conditional probability of finding a spin-σ electron at the position r provided that two spin-σ' electrons are fixed at the positions r_1 and r_2 (it can also be interpreted as a double conditional probability). The obtained results for $\rho(r_\downarrow,r_{1\uparrow},r_{2\uparrow})$ are shown in Fig. 11 after selecting, among over 10 million configurations sampled by the final DMC distribution, those with two like-spin electrons falling in predefinite positions and gathering the statistics over the relative ones of the remaining two particles.

As previously mentioned, the exact diagonalization yields a ground state with zero total-spin third component S_z, whereas the QMC and LSDA calculations predict a beryllium CDQR ground state, respectively, with $S=1$ and $S_z=1$. For LSDA, this can be seen from Fig. 12, in which we show the corresponding single-particle energy levels. However, we want to stress that the LSDA energy difference between the $S_z=2$ and $S_z=1$ configurations is about 0.06%, thus both being almost degenerate. Analogously, considering the results of Table IV, the QMC energies for the states $[L=0,S=0]$ and $[L=0,S=1]$ differ only by 0.01% to 0.2%, indicating a near degeneracy. This picture is corroborated by the one- and two-body densities and the angular modulation profiles for $[L=0,S=1]$ (not reported here), which look qualitatively the same as those shown for $[L=0,S=0]$.

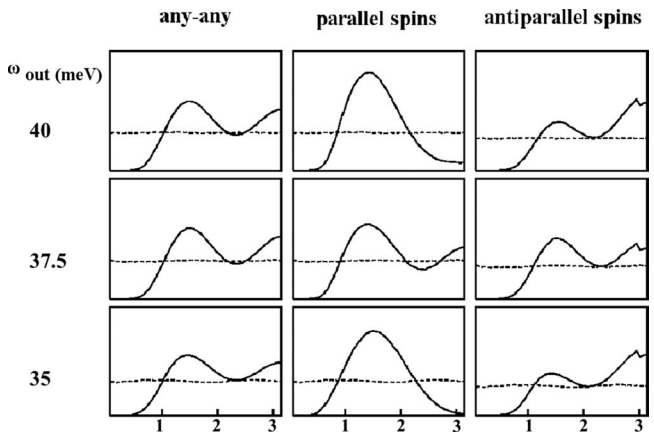

FIG. 10. Angular modulation of the density (arbitrary units) for the system with $N=4$ as a function of the relative angular distribution in radians. The dashed line shows the angular distribution of the one-body density, in arbitrary units but at the same scale as the angular modulations.

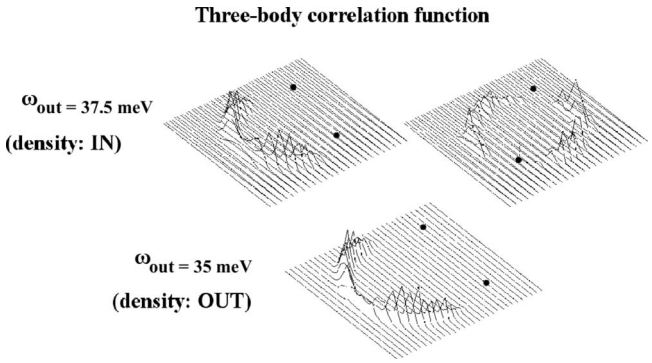

FIG. 11. Three-body correlation function for the beryllium CDQR; the dots show the positions of the two spin-up reference electrons.

It is worth pointing out that for the beryllium CDQR r_s ranges between 2 and 3 ($r_s=2.5$ when the four electrons are in the inner ring and $r_s=3$ when they are in the outer one). Such values are remarkably small as compared to those at which Wigner crystallization appears in the bulk system[28] and in quantum dots (near 20 for spin-polarized electrons[11]). This fact can be justified on the basis that the external potential used for CDQRs has a lower symmetry than the one used for QDs, therefore it favors the localization of the particles, as it generally happens for other low-dimensional electronic arrangements (see, e.g., Ref. 39).

IV. SUMMARY AND OUTLOOK

In this paper we have provided a systematic analysis and comparison of the ground-state energies of CDQRs containing $N=2-4$ electrons using quantum Monte Carlo, local spin-density approximation, and exact diagonalization meth-

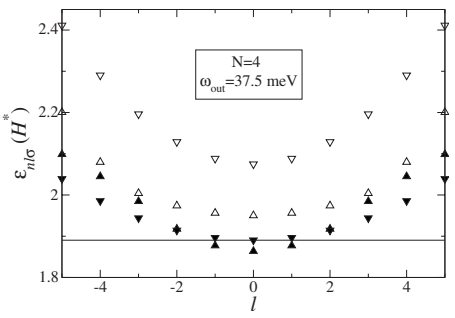

FIG. 12. Single-particle energy levels (in H^* units) of the LSDA calculation for the beryllium CDQR with $\omega_{out}=37.5$ meV. Up (down) triangles represent spin-up (down) states, the solid (open) ones corresponding to orbitals with principal quantum number $n=0$ ($n=1$). The horizontal line indicates the Fermi energy.

TABLE IV. QMC energies for the beryllium ($N=4$) CDQR in the $[L=0,S=1]$ state. Comparison with corresponding energies of Table III indicates that the ground state has $S=1$, thus obeying Hund's (first) rule.

ω_{out} (meV)	VMC (H^*)	DMC (H^*)
40 (IN)	6.7214(10)	6.6577(3)
37.5 (IN)	6.744(3)	6.6567(2)
35 (OUT)	6.4124(9)	6.3861(8)

ods. Also, the one-, two- and three-body densities have been calculated in order to assess the occurrence of Wigner crystallization in the intrinsic frame of reference of the systems. The results obtained by quantum Monte Carlo and the exact diagonalization show a substantial agreement, ruling out the possibility that the features observed might be attributed to artifacts of the calculations.

Due to the chosen external potential and the small number of electrons, we have found that for all the studied cases, the electrons are mostly localized in one of the two rings, showing a clear tendency to arrange themselves with a relative angular modulation, as well as a finely tunable crossover of the density from one ring to the other without altering the rotating Wigner-molecule character of the system revealed by the two-body density, thus proving that the electrons are relatively localized even for the considered values of r_s, which are as small as 2.5. The crossover effect can be further studied, in particular adding a magnetic field perpendicular to the CDQR,[8] whose tunability can be experimentally produced more easily than acting on the external confinement, and which can act as a crossover switch. We have already verified this possibility within LSDA. This might eventually be seen as a controllable quantum behavior worthwhile for nanoelectronic applications.

ACKNOWLEDGMENTS

We would like to thank C. J. Umrigar for providing us with the CHAMP package, A. Emperador and J. M. Escartín for insights into the ED code, and M. Barranco and E. Lipparini for helpful discussions. This work was performed under Grant No. 2005SGR00343 from Generalitat de Catalunya and Grant No. FIS2008-00421/FIS from DGI, Spain (FEDER).

[1] L. Jacak, P. Hawrylak, and A. Wójs, *Quantum Dots* (Springer, Berlin, 1998).
[2] T. Chakraborty, *Quantum Dots* (Elsevier, Amsterdam, 1999).
[3] D. Bimberg, M. Grundmann, and N. N. Ledentsov, *Quantum Dot Heterostructures* (Wiley, Londres, 2001).
[4] E. Lipparini, *Modern Many-Particle Physics* (World Scientific, Singapore, 2008).
[5] S. M. Reimann and M. Manninen, Rev. Mod. Phys. **74**, 1283 (2002).
[6] T. Mano, T. Kuroda, S. Sanguinetti, T. Ochiai, T. Tateno, J. Kim, T. Noda, M. Kawabe, K. Sakoda, G. Kido, and N. Koguchi, Nano Lett. **5**, 425 (2005).
[7] T. Kuroda, T. Mano, T. Ochiai, S. Sanguinetti, K. Sakoda, G. Kido, and N. Koguchi, Phys. Rev. B **72**, 205301 (2005).
[8] A. Mühle, W. Wegscheider, and R. J. Haug, Appl. Phys. Lett. **91**, 133116 (2007).
[9] R. C. Ashoori, H. L. Stormer, J. S. Weiner, L. N. Pfeiffer, S. J. Pearton, K. W. Baldwin, and K. W. West, Phys. Rev. Lett. **68**, 3088 (1992).
[10] S. Tarucha, D. G. Austing, T. Honda, R. J. van der Hage, and L. P. Kouwenhoven, Phys. Rev. Lett. **77**, 3613 (1996); F. Pederiva, C. J. Umrigar, and E. Lipparini, Phys. Rev. B **62**, 8120 (2000); **68**, 089901(E) (2003); L. Colletti, F. Pederiva, E. Lipparini, and C. J. Umrigar, Eur. Phys. J. B **27**, 385 (2002).
[11] A. D. Güclü, A. Ghosal, C. J. Umrigar, and H. U. Baranger, Phys. Rev. B **77**, 041301(R) (2008).
[12] R. Egger, W. Häusler, C. H. Mak, and H. Grabert, Phys. Rev. Lett. **82**, 3320 (1999).
[13] V. Halonen, P. Pietiläinen, and T. Chakraborty, Europhys. Lett. **33**, 377 (1996).
[14] M. Aichinger, S. A. Chin, E. Krotscheck, and E. Räsänen, Comput. Mater. Sci. **34**, 188 (2005).
[15] A. Fuhrer, S. Lüscher, T. Ihn, T. Heinzel, K. Ensslin, W. Wegscheider, and M. Bichler, Nature (London) **413**, 822 (2001).
[16] F. R. Waugh, M. J. Berry, D. J. Mar, R. M. Westervelt, K. L. Campman, and A. C. Gossard, Phys. Rev. Lett. **75**, 705 (1995); T. Schmidt, R. J. Haug, K. v. Klitzing, A. Förster, and H. Lüth, *ibid.* **78**, 1544 (1997); G. Schedelbeck, W. Wegscheider, M. Bichler, and G. Abstreiter, Science **278**, 1792 (1997); R. H. Blick, D. Pfannkuche, R. J. Haug, K. v. Klitzing, and K. Eberl, Phys. Rev. Lett. **80**, 4032 (1998); M. Brodsky, N. B. Zhitenev, R. C. Ashoori, L. N. Pfeiffer, and K. W. West, *ibid.* **85**, 2356 (2000); A. Lorke and R. J. Luyken, Physica B **256-258**, 424 (1998); M. Bayer, P. Hawrylak, K. Hinzer, S. Fafard, M. Korkusinski, Z. R. Wasilewski, O. Stern, and A. Forchel, Science **291**, 451 (2001); M. Pi, A. Emperador, M. Barranco, F. Garcias, K. Muraki, S. Tarucha, and D. G. Austing, Phys. Rev. Lett. **87**, 066801 (2001).
[17] F. Suárez, D. Granados, M. L. Dotor, and J. M. García, Nanotechnology **15**, S126 (2004); D. Granados, J. M. García, T. Ben, and S. I. Molina, Appl. Phys. Lett. **86**, 071918 (2005).
[18] B. Szafran and F. M. Peeters, Phys. Rev. B **72**, 155316 (2005).
[19] D. M. Ceperley and B. J. Alder, Phys. Rev. Lett. **45**, 566 (1980); J. W. Moskowitz, K. E. Schmidt, M. A. Lee, and M. H. Kalos, J. Chem. Phys. **77**, 349 (1982); P. J. Reynolds, D. M. Ceperley, B. J. Alder, and W. A. Lester, *ibid.* **77**, 5593 (1982); S. Fahy, X. W. Wang, and S. G. Louie, Phys. Rev. B **42**, 3503 (1990); X.-P. Li, D. M. Ceperley, and R. M. Martin, *ibid.* **44**, 10929 (1991); A. J. Williamson, J. C. Grossman, R. Q. Hood, A. Puzder, and G. Galli, Phys. Rev. Lett. **89**, 196803 (2002).
[20] M. H. Kalos and F. Pederiva, Phys. Rev. Lett. **85**, 3547 (2000).
[21] C. J. Umrigar, J. Toulouse, C. Filippi, S. Sorella, and R. G. Hennig, Phys. Rev. Lett. **98**, 110201 (2007).
[22] F. Malet, M. Barranco, E. Lipparini, R. Mayol, M. Pi, J. I. Cli-

mente, and J. Planelles, Phys. Rev. B **73**, 245324 (2006).
[23] M. Rontani, C. Cavazzoni, D. Bellucci, and G. Goldoni, J. Chem. Phys. **124**, 124102 (2006).
[24] I. Romanovsky, C. Yannouleas, and U. Landman, Phys. Rev. Lett. **93**, 230405 (2004).
[25] C. Yannouleas and U. Landman, Rep. Prog. Phys. **70**, 2067 (2007).
[26] J. Toulouse and C. J. Umrigar, J. Chem. Phys. **126**, 084102 (2007).
[27] F. Malet, M. Pi, M. Barranco, E. Lipparini, and Ll. Serra, Phys. Rev. B **74**, 193309 (2006).
[28] B. Tanatar and D. M. Ceperley, Phys. Rev. B **39**, 5005 (1989).
[29] A. Emperador, E. Lipparini, and F. Pederiva, Phys. Rev. B **72**, 033306 (2005).
[30] R. B. Lehoucq, K. Maschhoff, D. C. Sorensen, and C. Yang, ARPACK computer code, 1997, available at http://www.caam.rice.edu/software/ARPACK/
[31] K. Varga, P. Navratil, J. Usukura, and Y. Suzuki, Phys. Rev. B **63**, 205308 (2001).
[32] C. Herring, Phys. Rev. B **11**, 2056 (1975).
[33] J. Usukura, Y. Saiga, and D. S. Hirashima, J. Phys. Soc. Jpn. **74**, 1231 (2005).
[34] Y. Saiga, D. S. Hirashima, and J. Usukura, Phys. Rev. B **75**, 045343 (2007).
[35] S. A. Mikhailov, Phys. Rev. B **65**, 115312 (2002).
[36] M. Koskinen, M. Manninen, and S. M. Reimann, Phys. Rev. Lett. **79**, 1389 (1997).
[37] The matching of the number of maxima in the electron density with the number of electrons in the system has been followed as the criterion for Wigner crystallization in quantum dots, e.g., by E. Räsänen, H. Saarikoski, M. J. Puska, and R. M. Nieminen, Phys. Rev. B **67**, 035326 (2003).
[38] K. Hirose and N. S. Wingreen, Phys. Rev. B **59**, 4604 (1999).
[39] L. Shulenburger, M. Casula, G. Senatore, and R. M. Martin, Phys. Rev. B **78**, 165303 (2008).